# Multiscale analysis of hierarchical flax-epoxy biocomposites with nanostructured interphase by xyloglucan and cellulose nanocrystals

Estelle Doineau, Monica Francesca Pucci, Bernard Cathala, Jean-Charles Bénézet, Julien Bras, Nicolas Le Moigne

# Multiscale analysis of hierarchical flax-epoxy biocomposites with nanostructured interphase by xyloglucan and cellulose nanocrystals

Estelle Doineau [a,c,d], Monica Francesca Pucci [b,*], Bernard Cathala [c], Jean-Charles Benezet [a], Julien Bras [d,e], Nicolas Le Moigne [a,*]

[a] Polymers, Composites and Hybrids (PCH), IMT Mines Ales, Ales, France[1]
[b] LMGC, IMT Mines Ales, Univ Montpellier, CNRS, Ales, France[1]
[c] INRAE, UR BIA, F-44316, Nantes, France[1]
[d] Univ. Grenoble Alpes, CNRS, Grenoble INP, LGP2, F-38000 Grenoble, France[1]
[e] Institut Universitaire de France (IUF), F-75000 Paris, France

A B S T R A C T

Natural biological systems feature hierarchical nanostructured architectures achieving high strength and toughness. In this work, the spontaneous adsorption of xyloglucan (XG) and cellulose nanocrystals (CNC) onto flax fabrics is considered to develop hierarchical interphases with improved interfacial adhesion in epoxy-based biocomposites. A multi-scale analysis is carried out, from the nano & micrometric scale with the characterization of fibre surface topography, work of adhesion and interfacial shear strength (IFSS) between flax fibres and epoxy resin, to the macroscopic scale with the transverse mechanical properties of biocomposites. At the fibre scale, XG and CNC increase the surface roughness of flax fibres, as well as their adhesion to epoxy resin with IFSS improved by 60 %, up to 22.3 MPa. At the composite scale, the treatments have a major influence on the cohesion of flax cell walls and microstructure of the biocomposites. Transverse tensile tests reveal both cohesive and adhesive interfacial failure.

*Keywords:*
A. Biocomposite
A. Nano-structures
B. Interface/interphase
D. Microstructural analysis

## 1. Introduction

Performance and macroscopic properties of fibre-reinforced polymer composites are governed by many parameters related to the intrinsic properties of the matrix and fibres but also to the manufacturing process and the quality of the fibre / matrix interface [1]. In the case of biocomposites reinforced with plant fibres, several types of interfaces should be considered [2–4]: *(i)* the interface between the polymer matrix and the individualized elementary fibres and/or the fibres bundles, *(ii)* the interface between the elementary fibres within the fibre bundles, so-called middle lamella, and *(iii)* the interface between the layers constituting the cell walls. The fibre / matrix interfacial adhesion can be improved through three main strategies [5]: *(i)* modifying the surface free energy of the fibres and their polar and dispersive components impacts directly the work of adhesion with the matrix and thus favour their wetting and impregnation with the molten or liquid matrix during processing; *(ii)* developing (physical-)chemical functionalization of the fibres or adding coupling agents within the matrix can enhance the interfacial bonding by stronger (physical-)chemical interactions; (iii) increasing the interfacial area by the better dispersion of the fibres within the matrix and by changing the topography and/or the specific surface area of fibres can increase the mechanical interlocking with the matrix.

Following these strategies, various pre-treatments (e.g. retting, defibrillation process, solvent extractions) [3,6], chemical functionalization (e.g. silanes, NaOH, acid anhydrides) [7–10], plasma treatments [11] and/or thermal treatments [12] of flax fibres have been studied to increase the compatibility and bonding between flax fibres and epoxy matrix and hence the interfacial adhesion [5,13,14]. Those works obtained substantial improvements in the mechanical properties of flax / epoxy composites, until + 35 % in tensile strength and + 45 % in Young's modulus [15].

As recently reviewed by Doineau et al. [16], a new concept inspired by the structure of biological systems (bones, nacre, wood) consists in creating hierarchical fibres by depositing nano-objects on their surface (carbon nanotubes, ZnO nanowires, graphene, nanoclay, $TiO_2$ or

* Corresponding authors.
*E-mail addresses:* monica.pucci@mines-ales.fr (M. Francesca Pucci), nicolas.le-moigne@mines-ales.fr (N. Le Moigne).
[1] C2MA, LGP2 and BIA are members of the European Polysaccharide Network of Excellence (EPNOE) *http://www.epnoe.eu*.

nanocellulose) in order to develop wider interphases with local interfacial reinforcement, and to improve the mechanical interlocking between fibres and matrix. This approach has been developed in fully synthetic hierarchical composites [17–20], hybrid hierarchical composites reinforced with either synthetic fibres modified with bio-based nanoparticles or natural fibres modified with synthetic or mineral nanoparticles [21–25], and hierarchical fully bio-based composites reinforced with natural fibres modified with bio-based nanoparticles [26]. The creation of hierarchical fibres by the growth or deposition/grafting of nanofillers at their surface induces modifications of the fibre surface topography [16,18], but also the surface free energy of the fibres and their polar and dispersive components. Hierarchical nanoclays / carbon fibres were developed with an increased surface root mean square (RMS) roughness from ~64 nm to ~103 nm measured by atomic force microscopy (AFM) on 1 μm × 1 μm area [18]. Basalt fibres coated with ZnO nanorods showed a lower surface energy of 23.8 mJ/m$^2$ compared to 32.3 mJ/m$^2$ for neat basalt fibres, with also a strong decrease of the polar component $\gamma_S^p$ from 14 to 4.2 mJ/m$^2$ [17]. The nanostructuration of fibres showed in most cases an increase in the interfacial shear strength (IFSS). For example, an increase of 40.5 % was observed for epoxy resin and nano-$TiO_2$ modified flax fibres (2.34 wt% of particle content) compared to untreated fibres [23]. Considering hierarchical fully bio-based composites, most of the works used bacterial cellulose (BC) as nano-objects and cellulose acetate butyrate (CAB) or poly (lactic acid) (PLA) [27–30] as matrix. The most promising result was obtained with PLA/BC-grafted sisal fibre biocomposites with longitudinal and transverse tensile strengths increased by 44 % and 68 %, respectively, compared to the untreated sisal / PLA biocomposite. Moreover, BC treatment on sisal fibres improved the interfacial adhesion with the PLA matrix, with IFSS values increasing from 12.1 ± 0.5 MPa to 14.6 ± 1.2 MPa. Some studies also deal with the nanostructuration of natural fibres via the deposition of cellulose nanocrystals (CNC) or cellulose nanofibrils (CNF) at the surface of hemp or flax fibres [31–35]. Filling and binding effects of CNC and CNF were observed on elementary fibres and bundles constituting flax or hemp yarns, tapes and mats [31–33]. Moreover, a huge improvement in modulus, tensile stress and tensile strain was obtained for CNC treated hemp yarns by 36.1 %, 72.8 % and 67.7 % respectively. Polypropylene (PP) biocomposites reinforced with CNC-sprayed hemp mats were also studied [33]. Increases of 15 % in tensile strength and 16 % in Young's modulus were obtained using 2 wt% CNC modified hemp mats. However, the impact of CNC on the interfacial adhesion between hemp fibres and PP was not studied. Other works investigated the modification of flax fibres by CNC and xyloglucan (XG), a hemicellulose used as a binding agent due to its strong affinity towards cellulose surfaces [36,37]. The results showed the creation of an extensible network XG/CNC at the flax fibre surface [35], which was used to modify short flax fibres / PP composites combined with the use of maleic anhydride-grafted polypropylene (MAPP) as coupling agent [34]. The work of adhesion was increased by 9.5 % with MAPP and CNC compared to the untreated PP/flax composite (determined with tensiometry measurements), and the work of rupture by 21.6 % with MAPP and XG/CNC (based on micro-mechanical tensile tests), compared to PP/MAPP/flax composite. Based on these results, the spontaneous adsorption of CNC or CNF on flax fibre surfaces appears to be an interesting approach to develop hierarchical interphases with enhanced interfacial adhesion.

In this context, this work proposes to investigate this approach in structural biocomposites, i.e. epoxy resin reinforced with flax woven fabrics. The impact of XG and CNC adsorption treatments of flax fabrics on flax / epoxy interfacial properties is studied through a multi-scale analysis: *(i)* from the nano & micrometric scale with the characterization of fibre surface topography, the work of adhesion and wettability, and the mechanical interfacial strength between elementary flax fibres and epoxy resin, *(ii)* to the macroscopic scale with the analysis of the transverse mechanical properties of flax fabrics / epoxy biocomposites. The results are discussed in relation to the microstructure, i.e. fibre dispersion, fibre volume fraction and porosity, of the manufactured biocomposites.

## 2. Materials and methods

### 2.1. Materials

Unidirectional (UD) flax woven fabric (areal weight of 300 g/m$^2$ according to manufacturer) was manufactured by Eyraud (France) and supplied by Fibres Recherche Développement (FRD, France). CNC were produced by acid hydrolysis of wood pulp and purchased from CelluForce in spray-dried powder (Quebec, Canada). The CNC surface charge density from sulfate ester groups is 0.023 mmol/g; the crystalline fraction (Segal method): 0.88; the CNC lateral dimensions: 2–5 nm; and the CNC length: 50–110 nm based on analysis of Transmission Electron Microscopy (TEM) images. XG Glyloid 6C was obtained from tamarind seed gum and purchased from DSP Gokyo Food & Chemical (Japan). $Mw$ = 840,000 g.mol$^{-1}$; $Mw/Mn$ = 1.24, $Rg$ = 72 nm; monosaccharide composition: Glucose 50.7 %; Xylose: 31.7 %; Galactose 16.0 %; Arabinose 1.6 %. Epoxy resin SR Infugreen 810 and hardener SD 4770 were provided by Sicomin (France); ratio 100/29 (g/g); $T_g$ = 97 °C; 16-hours curing cycle at 60 °C; viscosity is 142 mPa.s at 20 °C and a maximum bio-based carbon content of 29 % for the mix resin/hardener (according to manufacturer).

### 2.2. Treatment of flax woven fabrics with XG and CNC

CNC and XG were adsorbed onto UD flax woven fabrics. A CNC suspension was prepared, i.e. 26 g of CNC in 1.8 L deionized water under stirring for 5 h, corresponding to a ratio *CNC:flax* of *1:6.6*, followed by sonication to break residual CNC agglomerates. Then, 8 plies of 25 x 25 cm$^2$ flax fabrics were cut from a UD flax woven fabric roll, were laid flat in the CNC suspension and stored at 4 °C for 16 h to allow spontaneous adsorption of CNC onto flax fibres to occur. The resulting CNC modified flax fabrics were then washed carefully with deionized water to remove the non-adsorbed CNC and dried in a heat chamber at 60 °C overnight. The edges of the fabric were held together with tape to prevent the yarns of UD fabric from pulling apart. The same procedure was followed for the modification of flax fabrics with both XG and CNC. In this case, XG was first adsorbed onto flax fabrics as follows: XG solution was prepared, i.e. 34.8 g of XG added gradually in 2.8 L deionized water with a vortex, at 50 – 60 °C during few hours, corresponding to a ratio *XG:flax* of *1:5*. Then, 8 plies of flax fabrics were laid flat in an adequate container containing the XG solution and stored at 4 °C for 24 h to allow spontaneous adsorption of XG onto flax fibres to occur. The XG modified flax fabrics were then washed carefully with deionized water to remove the non-adsorbed XG and were then dipped in a suspension of CNC following the previous treatment protocol. In order to study the possible effect of the water soaking/washing steps on the structure of flax fabrics, a control material has been prepared, i.e. 8 plies of UD flax fabrics were dipped in deionized water (without XG/CNC) and stored at 4 °C for 24 h. Flax fabrics were then "washed" and dipped in a second deionized water in an adequate container and stored at 4 °C for 24 h. Finally, flax fabrics were then dried in a heat chamber at 60 °C overnight. The resulting untreated, control, CNC and XG/CNC modified flax fabrics, named *flax*, *flax_control*, *flax_CNC* and *flax_XG/CNC* respectively, were stored in a conditioning room at 23 °C and 50 % relative humidity before manufacturing the biocomposites.

### 2.3. Flax fibre surface topography: Atomic force microscopy (AFM)

The surface roughness of untreated and treated flax fibres was estimated using an Atomic Force Microscope (AFM). Elementary flax fibres were extracted from untreated and treated yarns, and each individualized fibre was attached to a sample holder with double-sided adhesive

tape for AFM experiments. Images were obtained in a tapping mode with the MFP-3D Infinity AFM (Asylum Research) using a silicon probe (AC160R3 from Asylum, stiffness of 26 N/m, resonance frequency of 300 kHz). Image parameters were as follows: scan rate of 1 Hz, scan size of 3 μm x 3 μm at a resolution of 256 x 256 pixels. The scan size was chosen according to the largest zone in flax surface without curvature changes due to the fibre cross-section. This change in curvature has an effect on topography, and therefore on roughness values, which must be taken into account [38]. At least 3 different images were taken per sample and the most representative AFM images were selected for discussion. The RMS roughness was determined on three different surface areas of fibre for each fibre type.

### 2.4. Work of adhesion: Single fibre tensiometry

Elementary flax fibres extracted from yarns modified with CNC and XG/CNC were used for these experiments. The tensiometer K100SF (Krss, GmbH) was used to perform wettability tests with different test liquids following the Wilhelmy method (see **Eq.** (1)):

$$F = m.g = \gamma_L.p.\cos\theta \quad (1)$$

With $F$ the capillary force (mN) measured by the tensiometer when a single fibre is immersed in the test liquid, $m$ (g) corresponding to the mass of the liquid meniscus formed around the immersed elementary fibre, $\gamma_L$ (mN/m) the liquid surface tension, $p$ (m) the fibre wetted length or perimeter and θ (°) the static advancing contact angle between the fibre and the liquid [39]. The parameters used for wettability tests are detailed in a previous work [34]. Additional experiments were performed in this study in order to characterize the wettability of flax fibres by the epoxy resin without the hardener used for composite manufacturing. Measurements were carried out on six fibres for each treatment type and test liquid.

### 2.5. Mechanical adhesion: IFSS measurement by microbond test

Fifteen elementary flax fibres were extracted from the four types of (un-)treated fabrics/yarns and positioned on a plastic tab before being quickly fixed, approximately 10 s, with a photo-curing glue (DYMAX, Wiesbaden, Germany). This step is crucial and prevents slippage of elementary fibres out of the plastic tab due to slight tension applied during measurements. A fibre dimensional analysis system (FDAS770, Diastron Ltd, Hampshire, UK) controlled by UvWin 3.60® software was used to measure the cross-sectional dimensions of elementary fibres. The nominal length was 20 mm and typical apparent diameters ranged from 10 to 25 μm. This experimental method based on automated laser scanning of the fibre, as well as the overall sample preparation protocol, has been well optimized and described in reference [40]. During the measurement, the elementary fibre is put under slight tension to maintain it straight, then translated and rotated, in order to collect about 200 values of apparent diameter per revolution for each cross-section. 20 cross-sections were measured along the fibre length, allowing to consider the irregularity and the non-circularity of their cross-section. Around five to ten epoxy resin droplets were placed on the elementary flax fibre by using a single glass fibre as pencil, previously dipped in the epoxy resin. Curing is then conducted, i.e. 16 h at 60 °C in an oven. Droplets deposited on elementary flax fibre were checked by optical microscopy (Laborlux 11, Leitz) to reject asymmetric droplets and droplets having a diameter higher than 150 μm to avoid fibre breakage. Embedded fibre lengths were also measured and then, elementary fibres under slight tension were cut at their centre to obtain two samples held on a plastic shelf on one side and free on the other, called “single-ended”. For each sample, one or two droplets were targeted for subsequent microbond tests. After the reject of some samples due to defaults, around fifteen fibres were mechanically tested by the IFSS mode of the microtensile LEX820 device, equipped with a load cell of 20 N and controlled by UvWin 3.60® software (Diastron Ltd., Hampshire, Royaume-Uni). The loading rate during debonding was 0.1 mm/min and tests conditions were around 40 %HR and 23 °C. The razor blade slit used was 50 μm, to allow the holding of the resin drop without damaging the flax fibre. Force–displacement plots were recorded during the test, in order to determine the debonding force $F_{max}$. and calculate the apparent shear strength $\tau_{app}$ known as the IFSS [41] (see **Equation (2)**):

$$\tau_{app} = IFSS = \frac{F_{max}}{S} \quad (2)$$

where the embedding surface (S) corresponds to the bonded area between the elementary fibre and the epoxy resin droplet and is calculated from the average perimeter of the fibre cross-section and the embedding length of the fibre in the droplet, determined by optical microscopy.

### 2.6. Manufacturing of biocomposites

8 plies of flax fabrics (*flax, flax_control, flax_CNC or flax_XG/CNC*) were dried in a heat chamber overnight at 60 °C in order to remove any residual water before composite manufacturing. The epoxy system was prepared with a 100 / 29 (g / g) ratio, i.e. 310 g of epoxy resin SR Infugreen 810 and 89.9 g of amine-based hardener SD 4770 and mixed with a wooden spatula for 5 min to homogenize the mixture. Each flax ply was removed from the heat chamber and directly impregnated by the hand lay-up technique with a silicon brush following the longitudinal direction of the yarns to avoid misalignment. Between each ply, a spiked roller was used to remove entrapped air bubbles between stacked flax plies. Then, the 8 impregnated and stacked plies were placed in a thermocompression press under various curing pressure and fixed curing temperature (60 °C) and time (16 h). The effect of curing pressure has been studied and optimal processing conditions were defined as 70 bars at 60 °C during 16 h. After processing, the composite laminates were cooled at ambient temperature for 2 h, demoulded and stored in a conditioning room (23 °C; HR = 50 %) before subsequent analysis

### 2.7. Microstructural analysis of biocomposites

The fibre (%$V_f$), matrix (%$V_m$) and porosity (%$V_p$) volume fractions were calculated using **Equations (3), (4) and (5)** [42]:

$$\%V_f = \%m_f \times \frac{\rho_c}{\rho_f} \quad (3)$$

$$\%V_m = \%m_m \times \frac{\rho_c}{\rho_m} \quad (4)$$

$$\%V_p = 100 - (\%V_f + \%V_m) \quad (5)$$

With %$m_f$ and %$m_m$ respectively the fibre and matrix mass fractions deduced from the areal densities of the composite plates and the 8 plies of UD flax woven fabric in the dry state (g/m$^2$); $\rho_f$, $\rho_m$ and $\rho_c$ the bulk densities of respectively flax fibre fabrics, epoxy resin and composite plates. Discs of 25 mm diameter were cut from UD flax / epoxy composite plates with a hole-saw and placed in an IR-balance (Precisa XM66) at 105 °C for 5 min to measure their areal density (g/m$^2$) in the dry state (three samples per plate). Bulk densities (g/m$^2$) were obtained in dry state (60 °C for one night) using a Gas pycnometer (Micromeritics AccuPyc 1330) in helium atmosphere. Densities of flax woven fabrics and epoxy resin were respectively 1.54 and 1.17 g/cm$^3$ (two samples per material).

In order to analyse the dispersion state and layout of flax yarns within the epoxy matrix in composite laminates, SEM observations were conducted on cross-sections cut in composite plates, perpendicular and parallel to the fibre direction, with a Quanta 200 FEG (FEI Company) under high vacuum at an acceleration voltage of 15 keV. These cross-sections were polished, and sputter coated with carbon using a

BALZERS CED 030 in order to ensure good surface conductivity and limit flax fibres degradation under the electron beam. For observations parallel to the fibre direction, cartographies of 3.5 mm x 12 mm consisting of 8 SEM images were built using the software Aztec® (Oxford Instruments). Moreover, the thickness of each composite plate has been measured with a calliper on three different locations.

### 2.8. Transverse tensile tests on biocomposites

Tensile properties were investigated on biocomposite laminates in the transverse direction, i.e. perpendicular to the fibre/yarn direction. Tensile tests were carried out using an MTS machine (Criterion C45.105) equipped with a force sensor of 100 kN and a MTS laser extensometer (LX500). Two reflective stripes were stuck on samples for the determination of the Young's modulus. According to NF EN 2747 standard, composite plates were cut to obtain specimens of 3 mm x 10 mm x 170 mm with a reference length between tensile jaws of 105 mm. The crosshead speed was fixed at 0.5 mm/min until a preload of 20 N and then 2 mm/min until the rupture of the sample. The tests were performed at 23 °C and 50 % relative humidity. Five samples were tested for each biocomposite laminate.

## 3. Results and discussions

### 3.1. Effect of treatments on the surface topography of elementary flax fibres

The treatment of flax fibres by the adsorption of XG and CNC at their surface has been the topic of our previous work [35], which was focused on the adsorption mechanisms and the physical–chemical interactions between flax fibres, XG and CNC. Using confocal microscopy and adsorption isotherms, this study demonstrated the beneficial effect of pre-adsorption of XG to ensure a high quantity of adsorbed CNC onto flax fibres (25–30 mg /$g_{fibres}$). This treatment is likely to have an impact on the local roughness of treated flax fibres and hence on the mechanical interlocking and interfacial adhesion with the epoxy matrix. In this regard, 3D-AFM images of 3 μm x 3 μm surface area of elementary raw flax fibres were obtained and have shown surface heterogeneities (Fig. 1). A grooved surface can be observed in Fig. 1**a**, which is related to the microfibrils from the primary (P) wall (or secondary S1 wall if the P wall was damaged upon the different flax processing steps). Such observations on raw flax fibres have already been reported in literature [43,44]. In contrast, the surface of another flax fibre in Fig. 1**b** extracted from the same fabric is completely different with asperities and deposits. Such surface topography has also been observed in literature [45,46], where asperities are attributed to amorphous polymers remaining middle lamellae, such as pectins. These polymers are easily removed by washing with water or ethanol, revealing in most cases the microfibrils [3,7,46]. The latter are still visible in Fig. 1**b** but largely covered by the surface deposits.

AFM topography and phase images of CNC, *flax, flax_CNC* and *flax_XG/CNC* elementary fibres have also been taken and are shown in Fig. 2. First, the oriented microfibrils at the surface of raw flax fibres identified in Fig. 2 **b and c** are also evident on the topography and phase images of CNC treated fibres (Fig. 2 **d and e**). Compared to raw flax fibres**,** several nano-sized rod-shaped objects are visible at the surface of the CNC treated fibre by phase contrast (Fig. 2 **e**) and are related to CNC adsorbed on the fibre surface during treatment of fabrics. The maximum surface rate of CNC adsorbed on 3 μm x 3 μm area from the elementary flax fibre surface was calculated and estimated at about $10^6$ CNC, considering CNC size of 2 – 5 nm lateral dimensions and 50 – 110 nm length, average elementary flax fibre diameter of 20 μm, a density of 1.5 g/$cm^3$ and the adsorption rate determined at around 25 $mg_{CNC}$ /$g_{fibre}$ in our previous study [35]. In reality, the adsorption is locally inhomogeneous, with CNC-free zones and aggregated CNC, considerably reducing the actual number of objects observed. In contrast, microfibrils are less evident on the surface of XG/CNC treated flax fibres with a surface covered by a flaky polymer film (Fig. 2 **f and g**), due to the presence of XG. Some rod-like shape objects are also visible in the topography and the phase images (Fig. 2 **f and g**) and are in some places mixed up with the XG polymer.

To complete these observations, the root mean square roughness of *flax, flax_control, flax_CNC* and *flax_XG/CNC* fibres have been determined as an average on three surface areas results per type of fibre. Average values and standard deviations are reported in Table 1. First, Balnois et al. [43] have shown in their work focused on flax fibres that the RMS roughness value was highly dependent on the scanned surface area over the fibres. Indeed, the larger the scan size, the higher the RMS roughness value, due to higher probability to find residues and deposits contributing to the increase of the overall roughness. For example, they found a RMS roughness value of 35 nm for a scan area of 25 $μm^2$, against 10 nm for a scan area of 1 $μm^2$. RMS roughness value of 17.7 ± 0.7 nm (reported in Table 1) has been found for raw flax fibres, which is lower than the 30 nm found in reference [43] for an identical scan size of 9 $μm^2$. Balnois et al. [43] characterized dew-retted and mechanically separated flax fibres, probably rougher than the fibres extracted from the woven flax fabric used in this work that has undergone washing and weaving operations, implying less deposits and residues at the surface of fibres. Besides, the soaking in water and drying steps of flax fabrics (*flax_control*) increases the RMS roughness up to 28.8 ± 1.1 nm (Table 1), 65 % higher than for the raw flax fibre. The adsorption of CNC and XG/CNC at the surface of fibres does not increase the overall surface roughness compared to the *flax_control*, with RMS values of 29.7 ± 3.2 nm and 28.3 ± 3.6 nm, respectively (Table 1). Nevertheless, more

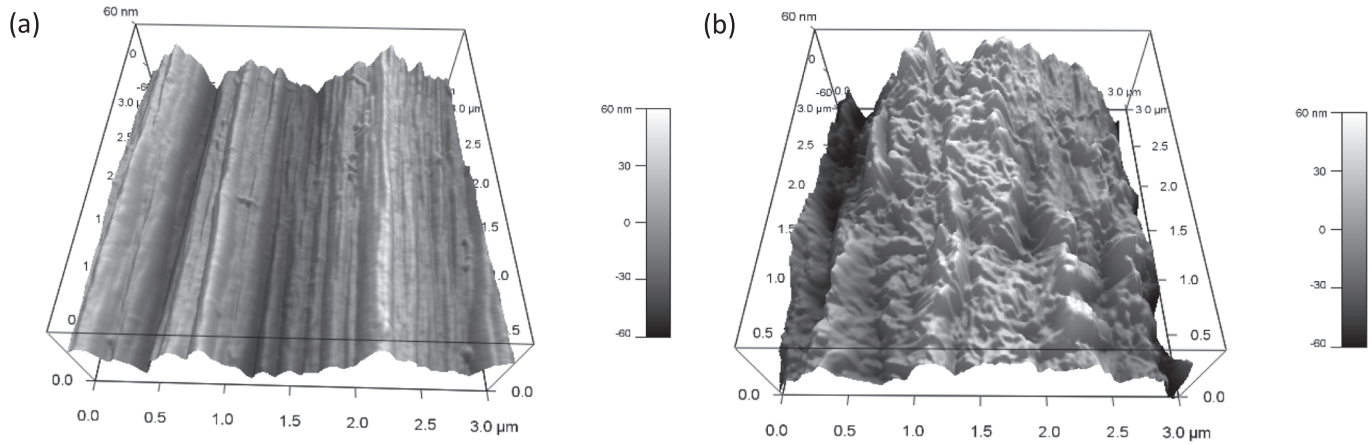


**Fig. 1.** 3D-AFM images (a) and (b) of the surface topography of elementary untreated flax fibres extracted from flax fabrics.

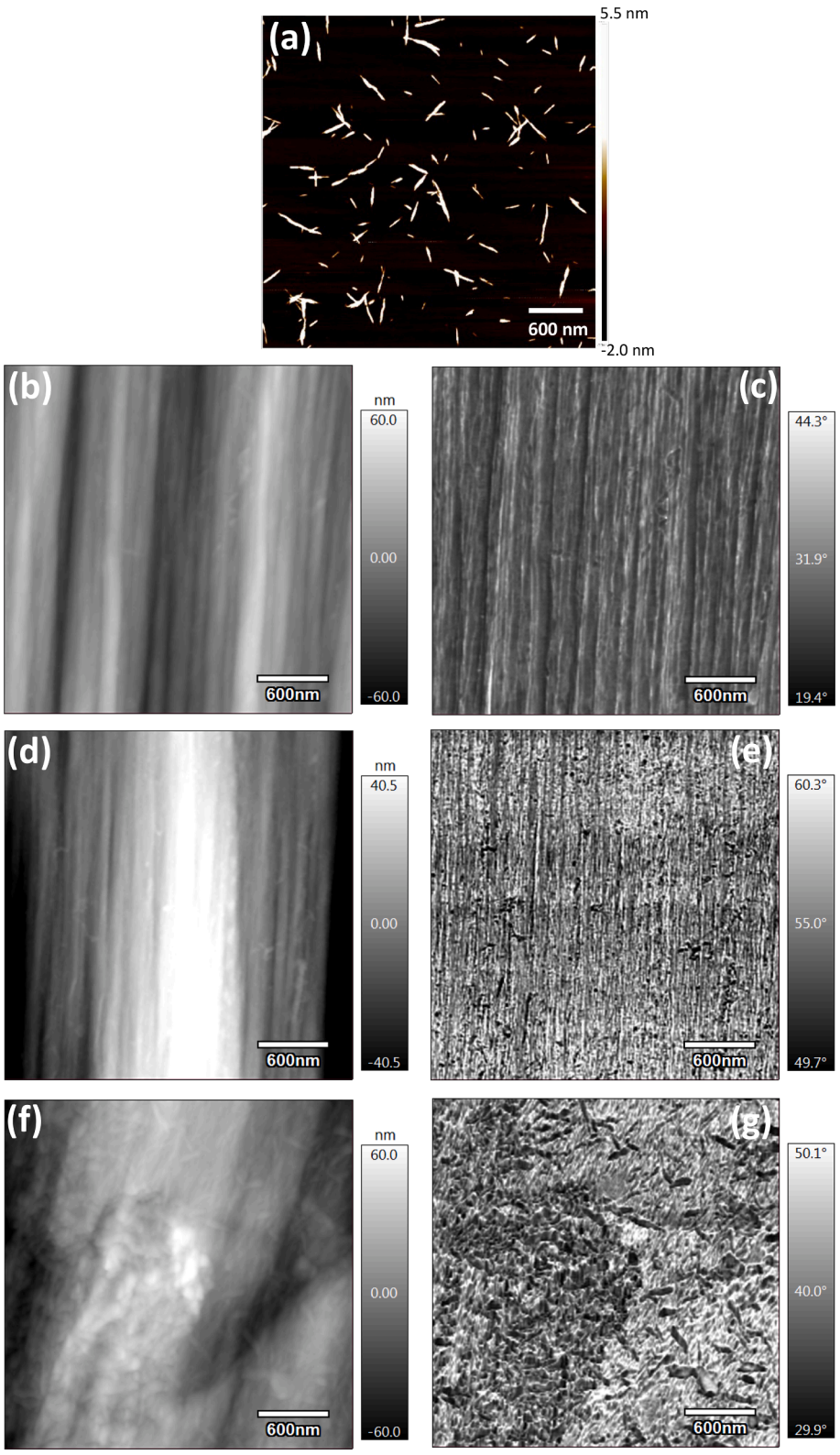


**Fig. 2.** AFM-topography image of (a) CNC; AFM-topography and AFM-phase images of (b – c) flax, (d – e) flax_CNC and (f – g) flax_XG/CNC fibre surface.

**Table 1**
RMS roughness of fibre surfaces measured by AFM.

| ***Samples*** | **Flax** | **Flax_control** | **Flax_CNC** | **Flax_XG/CNC** |
|---|---|---|---|---|
| RMS roughness (nm) | 17.7 ± 0.7 | 28.8 ± 1.1 | 29.7 ± 3.2 | 28.3 ± 3.6 |

scattered RMS values were found in the presence of CNC and XG/CNC, suggesting a possible local roughness. Indeed, at this scale, it exists several types of roughness: *(i)* the overall roughness measured on the scan surface area, primarily influenced by the topography of the fibre, and *(ii)* a local roughness influenced by the presence of little objects or defects at the surface of the fibre.

### 3.2. Interfacial adhesion between elementary flax fibres and epoxy resin

The adhesion features all the physical–chemical phenomena such as roughness and surface free energy of fibres, surface tension of matrix describing the wettability and the type of physical–chemical interactions between the fibres and the molten polymer matrix. The mechanical adhesion (or bonding) is related to the interfacial strength between fibres and matrix within the composite in the solid state during mechanical loading [47]. Therefore, the fibre / matrix interfacial adhesion is driven by the nature and strength of the interactions and the interfacial area.

#### 3.2.1. Work of adhesion

The surface free energy $\gamma_s$ of elementary flax fibres and its polar and dispersive components $\gamma_s^p$ and $\gamma_s^d$ (mJ/m$^2$) were determined by the Owens, Wendt, Rabel and Kaelble (OWRK) approach [48] knowing the respective polar and dispersive surface tensions of the test liquids $\gamma_L^p$ and $\gamma_L^d$ (mJ/m$^2$) (**Equation (6)**).

$$\frac{\gamma_L(1+\cos\theta)}{2\sqrt{\gamma_L^d}} = \sqrt{\gamma_S^p}\times\sqrt{\frac{\gamma_L^p}{\gamma_L^d}}+\sqrt{\gamma_S^d} \quad (6)$$

Surface free energies and its dispersive and polar components have been determined by single-fibre tensiometry and are reported in Table 2 for raw, control and treated flax fibres (*flax_CNC* and *flax_XG/CNC*). Surface tensions of test liquids are also reported in Table 2. Raw flax fibres have a surface free energy of 34.3 ± 3.3 mJ/m$^2$ with polar and dispersive components of 18.2 ± 3.1 mJ/m$^2$ and 16.1 ± 0.2 mJ/m$^2$, respectively. The effect of the soaking in water and drying steps (*flax_control* fibres) is limited with surface free energy of 34.4 ± 2.3 mJ/m$^2$ with polar and dispersive components of 17.8 ± 1.9 mJ/m$^2$ and 16.6 ± 0.4 mJ/m$^2$, respectively. A slight increase in the dispersive character is noticed, possibly due to the removal of amorphous hydrophilic polymers present at the surface of raw flax fibres (see Fig. 1 **b**). On the other hand, the treatment of flax fibre surfaces by CNC decreases their surface free energy by about 10 % (Table 2). This decrease could be related to the nanostructuration of flax fibre surfaces with the deposition of CNC inducing a modification of contact angles due to the increase of the local roughness and an enhancement of their specific surface area [49]. This trend has already been reported for the deposition of carbon nanotubes on carbon fibre surfaces [50]. In contrast, the XG/CNC treatment did not change the surface free energy of flax fibres, the latter being similar to raw and control flax fibres. Khoshkava and Kamal [51] reported for CNC a high surface free energy value of 68.9 mJ/m$^2$ with a predominant dispersive component, i.e. $\gamma_{CNC}^d$ = 40.9 mJ/m$^2$ and $\gamma_{CNC}^p$ = 28.0 mJ/m$^2$. Considering their high dispersive character, the adsorption of CNC on flax fibre surfaces appears to decrease strongly the polar character of raw flax fibres by 28 %, while the dispersive component is slightly increased from 16.1 ± 0.2 mJ/m$^2$ to 17.7 ± 0.1 mJ/m$^2$. In the case of flax_XG/CNC treated fibres, the polar and dispersive components are almost identical to *flax_control* fibres, suggesting that the presence of XG counterbalances the dispersive effect of CNC due to its pronounced polar character [52].

The wettability of flax fibres towards epoxy resin was further analysed by comparing the contact angles between raw and treated flax fibres and the liquid epoxy resin, and by calculating the work of adhesion $W_A$ in between. Values are reported in Table 2. Works of adhesion $W_A$, $W_A{}'$ and $W_A{}''$ (mJ/m2) between flax fibres and epoxy resin were respectively calculated by three different approaches: Young-Dupré equation [53–55] ($W_A$), **Equation (7)**, Owens, Wendt, Rabel and Kaelble (OWRK) approach [48] based on the geometric mean of dispersive and polar components of the liquid surface tension and solid surface free energy ($W_A{}'$), **Equation (8)** and Wu approach [56] based on the harmonic mean of dispersive and polar components of the liquid surface tension and solid surface free energy ($W_A{}''$), **Equation (9)**:

$$W_A = \gamma_L(1+\cos\theta) \quad (7)$$

$$W_A{}' = 2\times\left[\sqrt{\gamma_S^d\times\gamma_L^d}+\sqrt{\gamma_S^p\times\gamma_L^p}\right] \quad (8)$$

$$W_A{}'' = 4\times\left(\frac{\gamma_L^d\cdot\gamma_S^d}{\gamma_L^d+\gamma_S^d}+\frac{\gamma_L^p\cdot\gamma_S^p}{\gamma_L^p+\gamma_S^p}\right) \quad (9)$$

Where $W_A$, $W_A{}'$ and $W_A{}''$ refer to the work of adhesion between the epoxy resin and flax fibre surface, $\theta$ the contact angle in between, and $\gamma_L$ the surface tension of the epoxy resin (46.7 mN/m). Note that the spreading pressure was neglected as the contact angle between flax surface and epoxy is higher than 10° [55]. In OWRK and Wu approaches, $\gamma_s^p$ and $\gamma_s^d$ (mJ/m$^2$) refer to polar and dispersive components of elementary flax fibres knowing the respective polar and dispersive surface tensions of the test liquid $\gamma_L^p$ and $\gamma_L^d$ (mN/m).

According to the Young-Dupré approach (**Equation (7)**), the lower the contact angle and the higher the surface tension of the epoxy resin, the greater the wettability and the work of adhesion $W_A$ between flax fibres and epoxy matrix. Since the contact angles with the epoxy resin and the calculated work of adhesion $W_A$ (Table 2) are similar with or without CNC, the Young-Dupré approach does not allow to discriminate the effect of CNC. On the other hand, when considering the polar and dispersive components of the surface free energies via the OWRK (**Equation (8)**) and especially Wu (**Equation (9)** approaches, it appears that the CNC treatment improves the work of adhesion with epoxy resin, with $W_A{}''$ = 56.5 ± 0.3 mJ/m$^2$ (*flax_CNC*) versus $W_A{}''$ = 53.5 ± 0.5 mJ/m$^2$ (*flax*). In contrast, the adsorption of XG/CNC at flax fibre surface results in a higher contact angle with the epoxy resin and a lower work of adhesion $W_A$ compared to CNC adsorption. This is also supported by OWRK and Wu approaches, with $W_A{}'$ of 64.9 ± 2.1 mJ/m$^2$ and $W_A{}''$ of 54.1 ± 1.2 mJ/m$^2$ similar to raw flax fibres. Finally, it appears that *flax_control* fibres have higher affinity with the epoxy resin than raw flax fibres, i.e. the contact angle is decreased by 23 % from 65.2° ± 1.3 to 63.7° ± 2.5 (Table 2). The removal of some biopolymers present at the surface of flax fibres appears to have a beneficial effect on the wettability of flax fibres with the epoxy resin.

The results thus show that CNC surface treatment reduces the polar character of flax fibres while slightly increasing their dispersive character. This increases the work of adhesion with the epoxy resin based on the OWRK and Wu approaches. In contrast, the XG/CNC treatment has no significant effect on the work of adhesion with epoxy resin due to similar polar and dispersive components as raw flax fibres. The following section focuses on the effect of XG and CNC treatments on the

**Table 2**
Surface tensions of test liquids, surface free energies (with their polar and dispersive components) and the contact angle $\theta$ and work of adhesion between the epoxy resin and flax fibre surface ($W_A$, $W_A{}'$ and $W_A{}''$) for raw, control and treated flax fibres at 20 °C.

| **Surface tensions** | $\gamma_L^p$(mN/m) | $\gamma_L^d$(mN/m) | $\gamma_L$(mN/m) | |
|---|---|---|---|---|
| Water | 51.0 | 21.8 | 72.8 | |
| *n*-hexane | 0.0 | 18.4 | 18.4 | |
| diiodomethane | 2.3 | 48.5 | 50.8 | |
| Epoxy resin | 1.3 ± 1.0 | 45.4 ± 1.0 | 46.7 ± 1.1 | |
| **Surface free energies** | $\gamma_S^p$(mJ/m$^2$) | $\gamma_S^d$(mJ/m$^2$) | $\gamma_s$(mJ/m$^2$) | |
| Flax | 17.8 ± 3.1 | 16.6 ± 0.2 | 34.5 ± 3.3 | |
| Flax_control | 17.5 ± 1.9 | 17.1 ± 0.4 | 34.6 ± 2.3 | |
| Flax_CNC | 12.8 ± 1.3 | 18.1 ± 0.1 | 31.0 ± 1.4 | |
| Flax_XG/CNC | 17.5 ± 4.3 | 16.9 ± 0.5 | 34.4 ± 4.8 | |
| **Wettability** | $\theta$ (°) | $W_A$(mJ/m$^2$) | $W_A{}'$(mJ/m$^2$) | $W_A{}''$(mJ/m$^2$) |
| Flax | 65.2 ± 1.3 | 66.3 ± 1.1 | 64.5 ± 1.3 | 53.5 ± 0.5 |
| Flax_control | 63.7 ± 2.5 | 67.4 ± 1.8 | 65.3 ± 1.3 | 54.5 ± 0.9 |
| Flax_CNC | 65.6 ± 1.2 | 66.0 ± 2.5 | 65.5 ± 0.5 | 56.5 ± 0.3 |
| Flax_XG/CNC | 66.9 ± 1.6 | 65.0 ± 2.5 | 64.9 ± 2.1 | 54.1 ± 1.2 |

fibre/matrix mechanical adhesion.

### 3.2.2. *Flax / epoxy mechanical adhesion*

Microbond tests were performed with the deposition of epoxy resin microdroplets on untreated and treated flax fibres, and the resulting IFSS values are reported in Fig. 3 **a and b**. In the literature, flax / epoxy IFSS ranges from 13.2 ± 3.2 MPa for the Electra variety to 22.3 ± 2.1 MPa and 22.5 ± 1.5 MPa for the Hermes variety [57,58]. In our study, the average IFSS was 15.8 ± 3.5 MPa for raw flax fibres (Fig. 3 **a and b)**, which is thus consistent with literature. The IFSS values for *flax_control* reported in Fig. 3 **a and b** were divided into two different groups, representative of the two types of debonding observed. The Type 1 corresponds to an adhesive interfacial failure followed by sliding of the microdroplet along the fibre, whereas the Type 2 corresponds to a more cohesive interfacial failure with a partial peeling of fibre cell walls, the transverse intracellular cohesion being in this case the weak point [58]. In most cases, force – displacement curves were similar to the Type 1, whereas *flax_control* also behave as Type 2 with non-constant frictions (36 % of *flax_control* specimens) as shown in Fig. 3 **c**. This suggests that the washing and drying steps undergone by the fibres during treatment result in contrasted interfacial failure behaviours: *(i)* Type 1 with weak interfaces and low IFSS and interfacial work of rupture values of 12.1 MPa and 0.3 mJ, respectively, and *(ii)* Type 2 with much higher IFSS and interfacial work of rupture values of 24.1 MPa and 0.6 mJ, respectively, compared to 14.1 MPa and 0.4 mJ for raw flax fibres, due to the partial decohesion and peeling of fibre cell walls (see Fig. 3 **b and d**).

CNC and XG/CNC treatments greatly improve the IFSS by 58 % (*flax_CNC*) and 44 % (*flax_XG/CNC*) compared to raw flax fibres with median values of 22.3 MPa and 20.4 MPa, respectively, and significantly reduce the scattering of IFSS values compared to *flax_control* (Fig. 3 **a and b**). Force – displacement curves were all Type 1, with interfacial work of rupture of 0.32 mJ and 0.4 mJ for *flax_CNC* and *flax_XG/CNC* (Fig. 3 **d**), respectively, highlighting a more limited peeling effect and thus possible strengthening of the intracellular cohesion of flax cell walls with XG and CNC. The increase in flax / epoxy IFSS for *flax_CNC* and *flax_XG/CNC* also correlates with the increase in fibre surface roughness (RMS) measured by AFM (see Table 1), which promotes better mechanical interlocking and adhesion. Furthermore, the adsorption of XG as a "bio-based glue" between the flax fibre and CNC notably increases the interfacial work of rupture compared to *flax_CNC* (see Fig. 3**d**). This is due to the creation of an extensible XG/CNC network, as evidenced by adhesive force measurements by atomic force microscopy (AFM) in reference [35], capable of withstanding greater strains.

## 3.3. *Effect of treatments on biocomposite microstructure*

### 3.3.1. *Morphology of flax yarns and dispersion state in epoxy resin*

Flax fabrics are multi-scale reinforcements, made of yarns woven together, and composed of several elementary flax fibres gathered or not in bundles by the middle lamellae. In composite materials, the presence of bundles in the matrix indicates a lower degree of dispersion of flax fibres, which creates defects in the material and limits their reinforcing

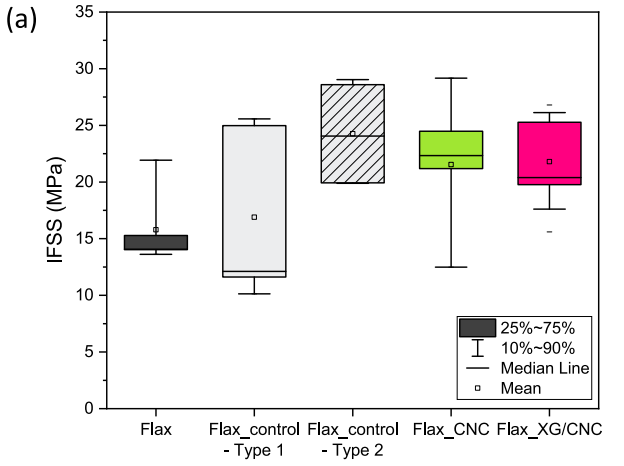


(b)

| | | IFSS (MPa) | | |
|---|---|---|---|---|
| | | Mean | Standard deviations | Median |
| **Flax** | | 15.8 | 3.5 | 14.1 |
| **Flax_control** | All | 19.6 | 7.1 | 20.0 |
| | Type 1 | 16.9 | 6.9 | 12.1 |
| | Type 2 | 24.3 | 5.0 | 24.1 |
| **Flax_CNC** | | 21.5 | 5.4 | 22.3 |
| **Flax_XG/CNC** | | 21.8 | 3.6 | 20.4 |

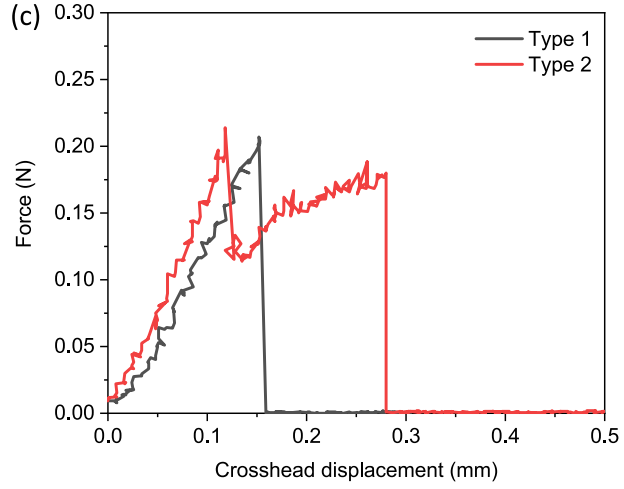


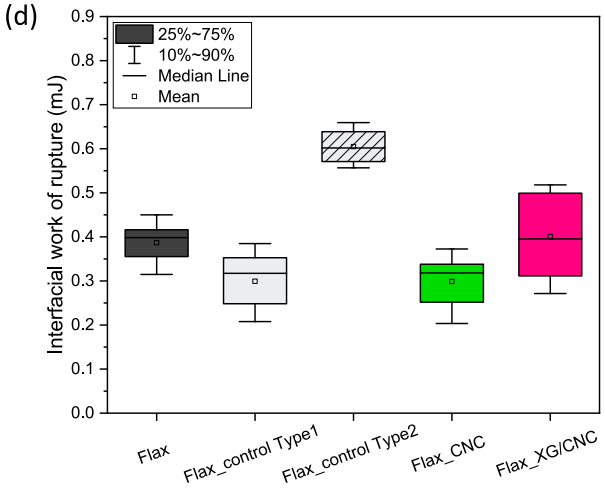


**Fig. 3.** (a) box charts of the IFSS measured by microbond tests with epoxy droplets on *raw flax*, *flax_control*, *flax_CNC* and *flax_XG/CNC* elementary fibres with (b) related mean and median values; (c) force–displacement curves with the two types of debonding behaviour observed with microbond tests; (d) box charts of the interfacial work of rupture.

effect of the fibres [59]. Indeed, it has been reported that failures occur preferentially within bundles when composites are subjected to mechanical stress. A better dispersion induces fewer fibre / fibre interactions and more elementary fibre / matrix interactions with enhanced interfacial area and mechanical interlocking [58].

SEM images of extracted flax yarns from fabrics (before composite manufacturing), as well as SEM images of polished cross-sections of flax / epoxy laminates at high magnification are shown (Fig. 4) for *raw flax*, *flax_control* and CNC and XG/CNC treated fabrics. Considering images of flax yarns, it seems that the XG/CNC treatment induces the creation of polymer web- or net-like structures surrounding the elementary fibres (Fig. 4 **d-left**). This was not observed for *raw flax*, *flax_control* and CNC treated flax fabrics, supporting that the presence of XG, possibly in higher amounts in some areas, is responsible for the formation of these polymer structures. This observation is in line with the resulting composite microstructure (Fig. 4 **d-right**), which shows a more packed structure made up of agglomerated elementary fibres in the case of XG/CNC treated fabrics. These agglomerated structures can be weak points and preferential sites of stress concentrations under mechanical stress inducing premature failures and cracks [59,60], which should be detrimental to the mechanical properties of composites. In contrast, raw, control and CNC treated flax yarns show a relatively good dispersion within the epoxy matrix (Fig. 4 **a, b and c**). Moreover, few voids are visible for *flax_control* / epoxy composite cross-sections with also a slightly better dispersion of elementary flax fibres, suggesting that water soaking tends to favour the fibre individualization within the yarns and during composite manufacturing.

CNC and XG/CNC and treatment (soaking, washing) processes thus influence the dispersion state of flax fibres within the manufactured biocomposites. The water soaking and drying of flax fabrics lead to microstructures with better dispersed fibres. On the other hand, the adsorption of biopolymers as XG having strong interactions with cellulosic surfaces [35] induces more packed structures with the formation or remaining of fibre bundles within the yarns, and poorer dispersion in epoxy matrix.

### 3.3.2. *Fibre volume fraction, porosity and packing*

Fibre $V_f$ and porosity $V_p$ volume fractions are strongly linked to the quality of impregnation of the fibres by the matrix and are key microstructural parameters that considerably influence the mechanical performance of composites. Basically, a high fibre volume fraction and low porosity result in better stiffness, strength and toughness [58,61,62]. The impregnation of flax fabrics with epoxy resin is a complex process as it involves different length-scale and multiple locations, i.e. around and within flax yarns, but also in between and within elementary fibres via the lumen cavity [63]. The quality of impregnation and resulting porosity is driven by many parameters, i.e. processing conditions, resin viscosity and its ability to wet flax fibres and the packing ability of flax fabrics. The porosity is multi-scale, including macro-pores that are generally caused by trapped gas bubbles or voids in the matrix, and micro-pores originating from the fibres themselves, interfacial porosity and poor impregnation inside the yarns [63,64].

The measured $V_f$ and $V_p$, determined according to **Equations (3)–(5)**, are presented in Fig. 5 for the different biocomposites. The raw flax fabric reinforced epoxy biocomposite has $V_f = 55.6$ % and $V_p = 2.4$ %. Using the same processing conditions for all biocomposites, it appears

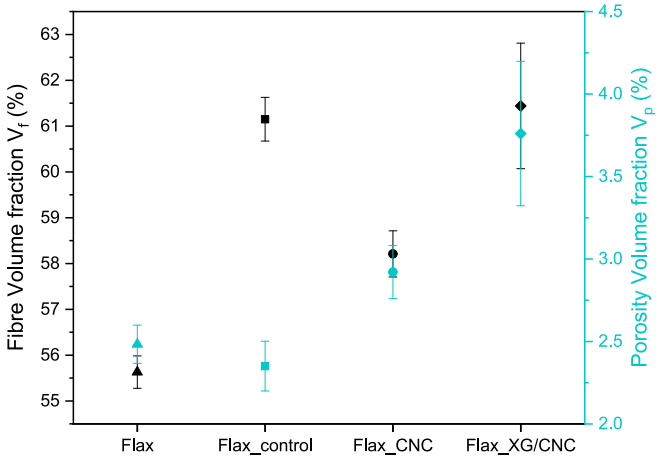


**Fig. 5.** Fibre volume fraction $V_f$ and porosity $V_p$ of *raw flax*, *flax_control*, *flax_CNC* and *flax_XG/CNC* fabrics reinforced epoxy biocomposites.

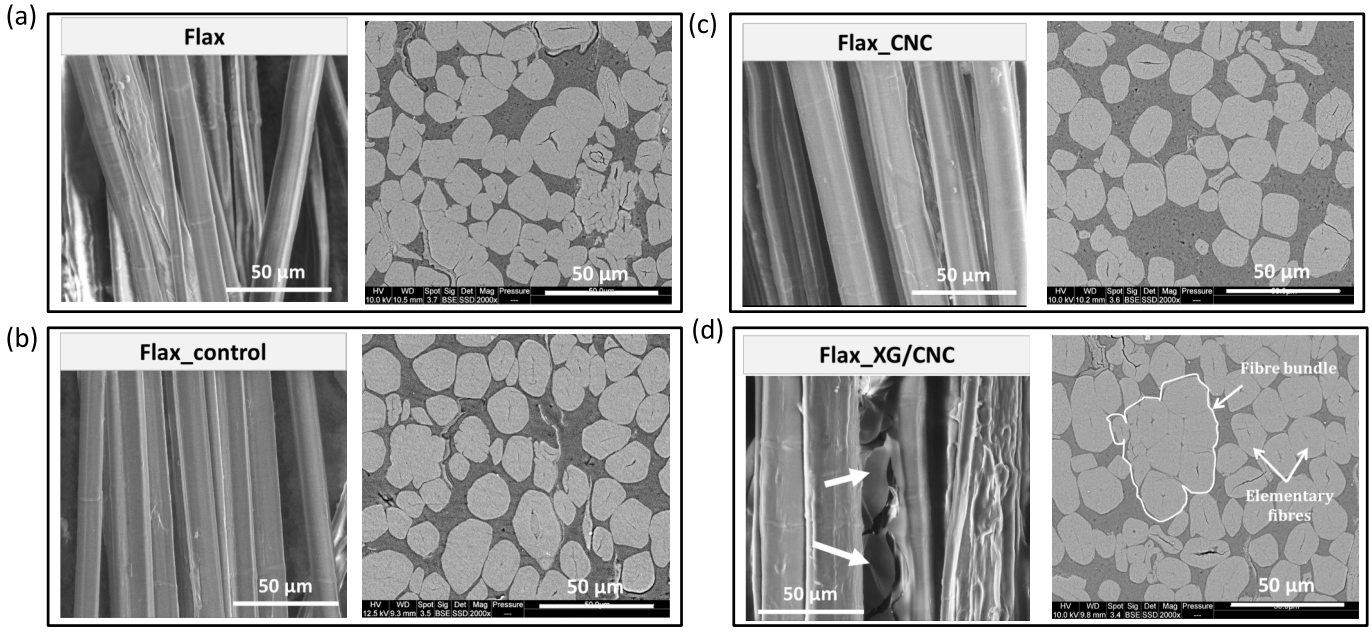


**Fig. 4.** On the left of black boxes: SEM images of extracted yarns from (a) raw, (b) control, (c) CNC and (d) XG/CNC treated flax fabrics; On the right of black boxes: SEM images of cross-sections of (a) raw, (b) control, (c) CNC and (d) XG/CNC flax / epoxy laminates. Flax bundles and elementary fibres appear in light grey, epoxy matrix in dark grey and porosities in black.

that the washing and drying steps have a positive impact with an increase of the fibre volume fraction up to 61.2 % with similar porosity ($V_p = 2.3$ %). The treatments of flax fabrics with CNC and XG/CNC also enhance the fibre volume fraction of composite plates up to 58.2 % and 61.5 %, respectively (Fig. 5). However, they also induce a slight increase in porosity for *flax_CNC* ($V_p = 2.9$ %), more pronounced for *flax_XG/CNC* ($V_p = 3.8$ %) (Fig. 5). Considering that processing conditions and resin physical–chemical characteristics (i.e. viscosity, surface tension, reactivity) remained unchanged for all biocomposites, the quality of impregnation and resulting $V_f$ and $V_p$ were thus mainly influenced by variations in the wettability of raw and treated flax fabrics. As supported by tensiometry experiments reported above, considering the resin contact angle and work of adhesion, the wettability of flax fibres with epoxy resin did not significantly change with the adsorption of CNC, while the presence of XG on flax fabrics appeared to increase slightly the contact angle and hence decrease the wettability with the epoxy matrix. This decreased wettability at the scale of elementary flax fibres by the XG/CNC treatment could partly explain the higher porosity measured for the corresponding biocomposite plate. The presence of web-like polymer structures (Fig. 4 **d-right**) between XG/CNC treated elementary fibres is also likely to affect the impregnation of flax yarns with the epoxy resin. Such packed structures are expected to prevent resin diffusion into the yarns and generate so-called "impregnation porosity" during biocomposite manufacturing [63], thus explaining the higher porosity in XG/CNC treated flax biocomposite.

Madsen et al. [63] pointed out that among other factors (lumen, interfacial adhesion, heterogeneous shape of natural fibres), the low packing ability of natural fibre fabrics is responsible for the creation of porosity. In particular, Madsen and Lilholt [64,65] observed that when increasing fibre weight fraction above an optimum value of about 52 wt % for polypropylene / flax composite, a decrease in Young's modulus and tensile strength is observed. The authors assumed that above this fibre weight fraction, the fibres / yarns reach their maximum packing ability, and that the balance between the fibre volume fraction and the occurrence of structural porosity induces an optimum in physical and mechanical properties of the composite. The increased porosity for CNC and XG/CNC treated biocomposites could thus originate from the higher fibre volume fractions in composite plates (Fig. 5), being above the maximum packing ability of the treated flax fabrics. Interestingly, using the same manufacturing conditions (pressure and temperature), the plate thicknesses for CNC and XG/CNC treatments are higher (3.09 ± 0.05 mm and 3.02 ± 0.06 mm respectively) than those obtained for raw and control flax fabrics (2.85 ± 0.01 mm and 2.82 ± 0.07 mm, respectively), supporting that CNC and XG/CNC treatments decrease the packing ability of flax fabrics. The lower thickness obtained with the control fabric indicates a higher packing ability and justifies the lower porosity ($V_p = 2.3$ %) of this composite while having the highest fibre volume fraction ($V_f = 61.2$ %). The packing ability of flax fabrics thus appears here to be a key factor influencing fibre volume fraction and porosity. More in-depth studies of porosity, given its multi-scale distribution, using other techniques such as X-ray tomography, would be interesting to better depict the effect of CNC and XG/CNC on interfacial and impregnation porosity [66–68].

Concluding, CNC and XG/CNC treatments strongly influence the fibre volume fraction and porosity of biocomposites even when manufactured in the same processing conditions. Higher fibre volume fractions up to 61.5 % were reached but overall porosity increased up to 3.8 % for the XG/CNC treatment. Beyond some variations in wettability at the scale of elementary fibres, the formation of fibre bundles within yarns due to XG and the decreased packing ability of treated flax fabrics are responsible for worse impregnation and substantial increase in porosity. This higher void content is likely to be detrimental for the mechanical properties of composite plates, especially their strength, because it could favour the initiation and propagation of microcracks.

### 3.4. Transverse mechanical properties of biocomposites

The mechanical properties of unidirectional flax fibres reinforced epoxy laminates have already been studied in literature using different manufacturing processes such as thermocompression, (vacuum-assisted) compression moulding, prepregging, autoclaving, liquid resin infusion or resin transfer moulding [6–8,58,61,69–79]. The authors obtained Young's modulus ranging from 15 GPa to 39 GPa and tensile strength ranging from 130 MPa to 415 MPa. Such large variations in mechanical performance are mainly related to differences in fibre volume fraction in the composites, the control of manufacturing processes, and also the type and quality of flax reinforcements [64,76,80]. In our work, longitudinal Young's modulus ranged from 30 GPa to 33 GPa and tensile strength from 270 MPa to 305 MPa for the different manufactured flax/epoxy laminates [15], attesting for their good mechanical properties, and hence the good control of the manufacturing process used.

In the transverse direction of UD fabric reinforced laminates, tensile strength is mostly determined by the matrix strength, the residual stresses, and the quality and quantity of fibre / matrix interfaces related to fibre content and dispersion state, and fibre / matrix interfacial adhesion [81]. Static transverse tensile tests conducted on UD fabric reinforced composites can thus highlight the interfacial adhesion and failure behaviour in the interphase zone [13]. Results of the transverse tensile tests on the different prepared biocomposites are represented in Fig. 6**.** Composites show a more ductile behaviour with a yield stress and plastic strain before breaking as compared to epoxy resin. The addition of CNC on flax fibres, decreases the transverse tensile strength by 22 %. It also induces a more brittle behaviour with a strong decrease of the breaking strain, as shown in Fig. 6 **a**. The treatment XG/CNC on flax fibres seems to have less impact on the transverse tensile strength with a decrease of 9.7 % compared to raw flax / epoxy composites (Fig. 6 **b**). In contrast, the *flax_control* / epoxy laminate displays higher transverse tensile strength with an increase of 11 % compared to the reference, which is attributed to better fibre dispersion, and thus enhanced fibre / matrix interfacial area as observed in Fig. 4 **b**. Values of transverse work of rupture follow the same trend as the transverse tensile strength with values of 0.88 ± 0.13 J, 1.02 ± 0.22 J, 0.38 ± 0.05 J and 0.37 ± 0.10 J (Fig. 6 **c**), for *raw flax, flax_control, flax_CNC* and *flax_XG/CNC* composites, respectively.

SEM images on fracture surfaces of transverse tensile flax / epoxy specimens are presented in Fig. 7. First, a peeling of flax cell walls has been observed for all specimens (Fig. 7 **a, b and c**). Many delaminated cell wall layers in the form of fibrillary ribbons were observed on failure surfaces, especially for the *flax_control* / epoxy laminate. Le Duigou et al. [57] studied the complex interphase zone between flax fibres and epoxy resin, and revealed via microbond tests a possible role of the resin penetration into the cell walls in the peeling phenomenon. Moreover, the authors highlighted in another study an increase of flax fibres fibrillation with the immersion time in water [82]. Indeed, the water soaking of flax fibres might induce a decrease of the intracellular cohesion within the cell wall structure of flax fibres. Furthermore, good interfacial adhesion between flax fibre surfaces and epoxy resin would also increase the peeling of fibres, if considering a weaker intracellular cohesion than fibre / matrix interfacial adhesion.

Moreover, different types of interfacial failures have been observed between flax / epoxy laminates (Fig. 7 **d, e and f**). Some residues of epoxy matrix are visible on untreated flax fibres (white arrow), indicative of cohesive interfacial failures but a major part of the fibres seems to be resin-free, supporting that the main mechanism was adhesive interfacial failure. In particular, the fibres treated with XG/CNC show very little matrix residue on their surface, which is consistent with an adhesive interfacial failure and the decreased tensile strength observed for the XG/CNC treated flax fibre composite (Fig. 6). Finally, the *flax_control* / epoxy laminate shows more chaotic fracture surfaces with a mix of epoxy resin and flax fibres (Fig. 7 **e**), hence supporting a better fibre / matrix adhesion in accordance with the higher transverse tensile

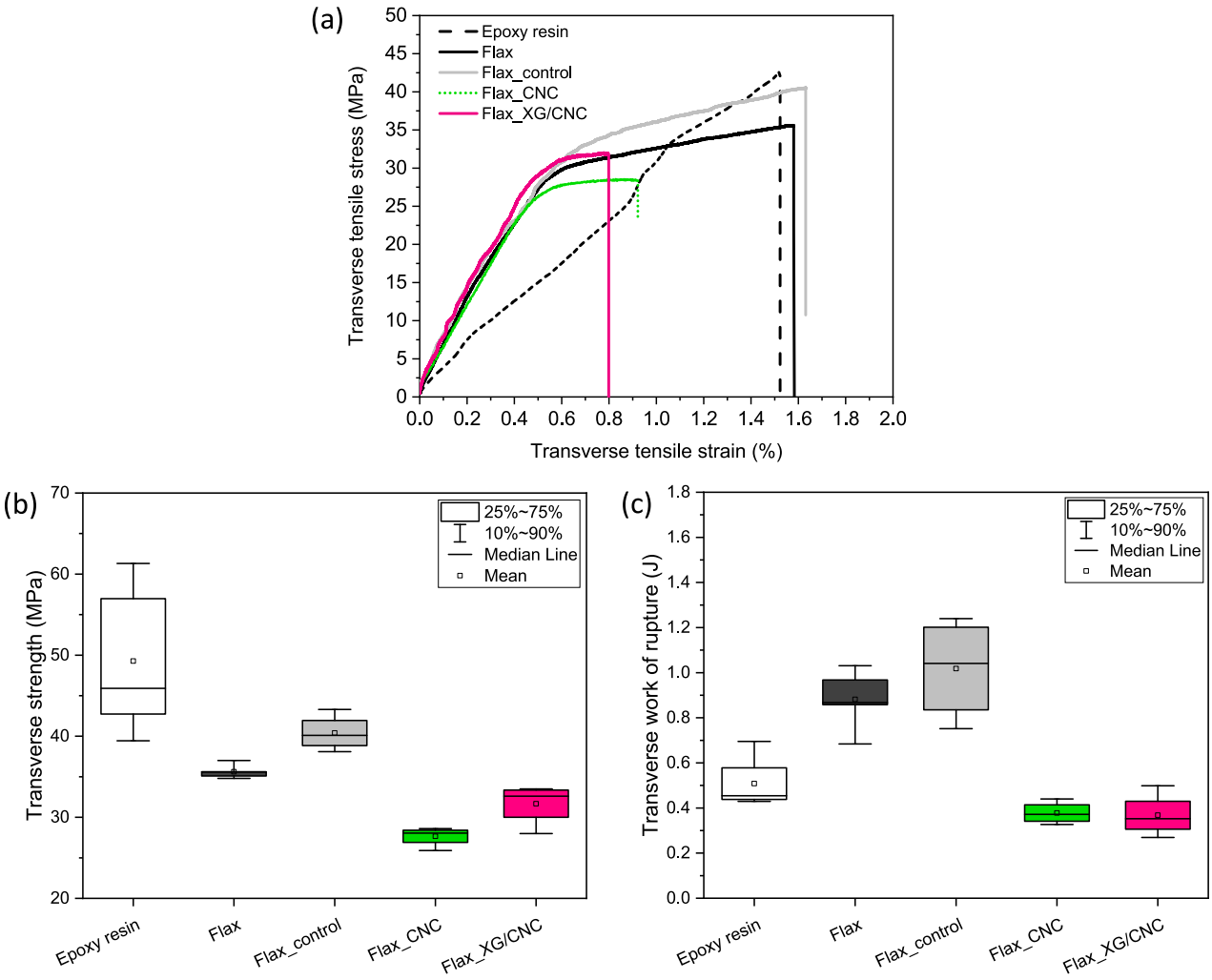


**Fig. 6.** Quasi-static transverse tensile properties for neat epoxy resin and the different biocomposite laminates (a) stress–strain curves, (b) tensile strength and (c) work of rupture.

strength and work of rupture of the composite. It should be pointed out that the cell wall peeling phenomenon described above could be partly responsible for these improved transverse tensile properties. Indeed, the peeled cell walls ribbons allow to dissipate more energy during failure and crack propagation, and sustain more load and strain, hence leading to higher work of rupture.

## 4. Conclusions

Hierarchical epoxy-based composites reinforced with XG/CNC modified flax fabrics have been developed and a multi-scale analysis of the interphase was conducted.

At the fibre scale, water soaking and drying steps (associated with the CNC and XG/CNC treatment process) of flax fabrics increase the surface roughness of flax fibres by 65 %, as well as the interfacial adhesion with the epoxy resin. Indeed, an increase of 16.8 % of the work of adhesion (Young-Dupré approach) as well as a decrease from 65.2° ± 1.3 to 63.7° ± 2.5 of the contact angle with the epoxy resin were measured. In addition, the median IFSS values measured by microbond test increased from 14.1 MPa to 20.0 MPa. Therefore, the removal of biopolymers from the surface of flax fibres by water soaking is beneficial for the flax/epoxy interfacial adhesion. On the other hand, water soaking favours the decohesion of flax fibre cell walls under mechanical stress. This peeling phenomenon improved the interfacial work of rupture as measured by microbond test. The CNC and XG/CNC treatments also increased the surface roughness of flax fibres as well as the work of adhesion (Wu approach) with epoxy resin, for the CNC treatment. Interestingly, the flax/epoxy IFSS could be further improved, 22.3 and 20.4 MPa respectively, with less scattered results. It is assumed that the presence of CNC and XG/CNC improves the cohesion of the fibre cell walls, thus limiting their peeling while contributing to improve flax / epoxy interfacial adhesion.

At the composite scale, fibre dispersion in epoxy resin was improved by the water soaking process. In contrast, the XG/CNC treatment results in more packed structures with the formation or remaining of fibre bundles. CNC and XG/CNC treatments also strongly influenced the fibre volume fraction and porosity in the composites, with higher fibre volume fraction up to 61.5 % but overall porosity increased up to 3.8 % for the XG/CNC treatment. Transverse tensile tests revealed different failure mechanisms with visible cell walls peeling, but primarily governed by adhesive interfacial failure. Higher transverse tensile strength and work of rupture were measured with the water-soaked flax fabrics. Beyond the hierarchical treatments of flax fibres with XG/CNC developed in this work, which have demonstrated their efficiency at the fibre scale, the naturally occurring hierarchical structure of flax cell walls, and its tailored destructuration (e.g. by water treatment) could be an advantage for controlling failure mechanisms and improving the mechanical strength of natural fibre reinforced composites.

In conclusion, improving the mechanical performance of biocomposite laminates reinforced with flax fabrics through interfacial

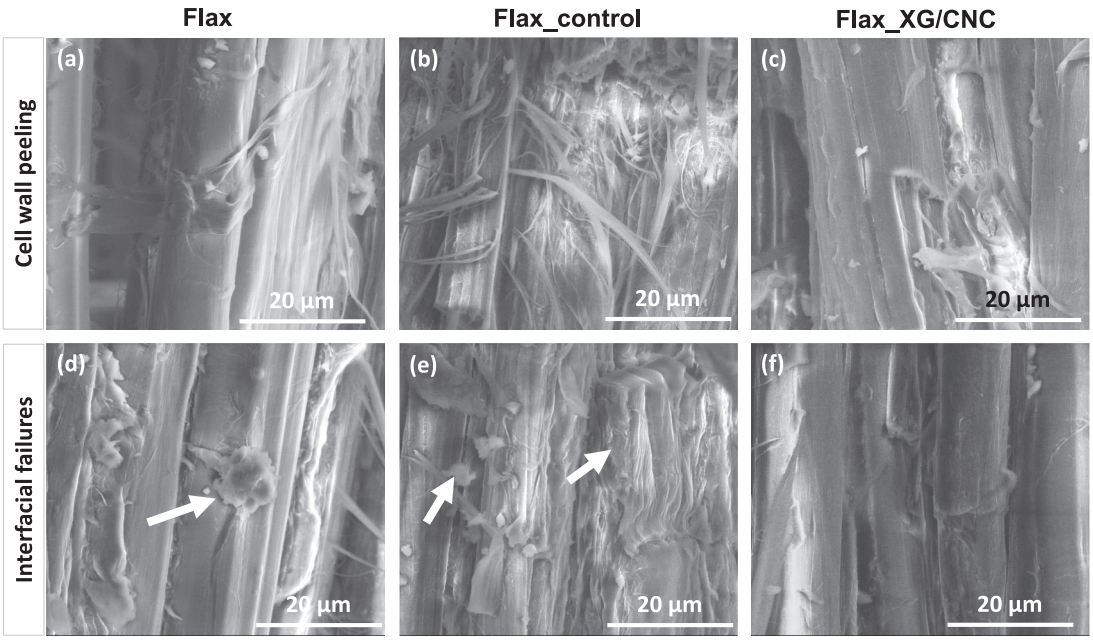


**Fig. 7.** SEM images of fracture surfaces observed after quasi-static transverse tensile tests on raw, control and XG/CNC treated flax fabrics / epoxy laminates with (a – c) the cell wall peeling phenomenon and (d – f) flax / epoxy interfacial failures (white arrows show epoxy matrix).

modifications appears as a great challenge, with the following key parameters to be controlled for the design of an optimal flax reinforcement: *(i)* Enhancing fibre / matrix interfaces via a better dispersion of flax fibres within the matrix while maintaining fibres / yarns orientation and integrity of the fabrics; *(ii)* Modifying fibre / matrix mechanical / chemical interactions via reactive molecules and nanostructuration while maintaining good fibre dispersion and good wettability towards the matrix; *(iii)* Exploring the controlled destructuration of the hierarchically organized flax cell walls to promote energy dissipation during crack propagation while maintaining the above-mentioned microstructural and wetting characteristics.

## CRediT authorship contribution statement

**Estelle Doineau:** Writing – review & editing, Writing – original draft, Visualization, Validation, Methodology, Investigation, Formal analysis. **Monica Francesca Pucci:** Writing – review & editing, Validation, Supervision, Methodology, Formal analysis. **Bernard Cathala:** Writing – review & editing, Validation, Supervision, Resources, Project administration, Methodology, Conceptualization. **Jean-Charles Benezet:** Writing – review & editing, Validation, Supervision, Project administration, Funding acquisition, Conceptualization. **Julien Bras:** Writing – review & editing, Validation, Supervision, Resources, Project administration, Methodology, Funding acquisition, Conceptualization. **Nicolas Le Moigne:** Writing – review & editing, Visualization, Validation, Supervision, Resources, Project administration, Methodology, Funding acquisition, Formal analysis, Conceptualization.

## Declaration of competing interest

The authors declare that they have no known competing financial interests or personal relationships that could have appeared to influence the work reported in this paper.

## Data availability

Data will be made available on request.


## Acknowledgements

Estelle Doineau thanks IMT Mines Alès and Doctoral School GAIA for funding her PhD work. A part of this work was supported by the French research cluster CNRS-INRA' Symbiose' SYnthon et Mat ériaux BIO-Sourcés for mission funding, and by Glyco@alps (ANR-15-IDEX-02), Idex UGA. LGP2 is part of the LabEx Tec 21 (Investissements d'Avenir – grant agreement n°ANR-11-LABX-0030) and of PolyNat Carnot Institute (Investissements d'Avenir – grant agreement n°ANR-16-CARN-0025- 01).


## References


[1] Müssig J, Haag K. The use of flax fibres as reinforcements in composites. In: Biofiber Reinforcements in Composite Materials. Elsevier; 2015. p. 35–85. https://doi.org/10.1533/9781782421276.1.35.

[2] Le Moigne N, Otazaghine B, Corn S, Angellier-Coussy H, Bergeret A. Interfaces in Natural Fibre Reinforced Composites: Definitions and Roles. In: Navard P, editor. Surfaces and Interfaces in Natural Fibre Reinforced Composites. Springer International Publishing; 2018. p. 23–34. https://doi.org/10.1007/978-3-319-71410-3_2.

[3] Acera Fernández J, Le Moigne N, Caro-Bretelle AS, El Hage R, Le Duc A, Lozachmeur M, et al. Role of flax cell wall components on the microstructure and transverse mechanical behaviour of flax fabrics reinforced epoxy biocomposites. Ind Crops Prod 2016:85. https://doi.org/10.1016/j.indcrop.2016.02.047.

[4] Bismarck A, Aranberri-Askargorta I, Springer J, Lampke T, Wielage B, Stamboulis A, et al. Surface characterization of flax, hemp and cellulose fibers; surface properties and the water uptake behavior. Polym Compos 2002;23:872–94. https://doi.org/10.1002/pc.10485.

[5] Le Moigne N, Otazaghine B, Corn S, Angellier-Coussy H, Bergeret A. Modification of the Interface/Interphase in Natural Fibre Reinforced Composites: Treatments and Processes. In: Navard P, editor. Surfaces and Interfaces in Natural Fibre Reinforced Composites. Springer International Publishing; 2018. p. 35–70. https://doi.org/10.1007/978-3-319-71410-3_3.

[6] Martin N, Davies P, Baley C. Comparison of the properties of scutched flax and flax tow for composite material reinforcement. Ind Crop Prod 2014;61:284–92. https://doi.org/10.1016/j.indcrop.2014.07.015.

[7] Huner U. Effect of chemical surface treatment on flax-reinforced epoxy composite. J Nat Fibers 2018;15:808–21. https://doi.org/10.1080/15440478.2017.1369207.

[8] Fiore V, Scalici T, Valenza A. Effect of sodium bicarbonate treatment on mechanical properties of flax-reinforced epoxy composite materials. J Compos Mater 2018;52:1061–72. https://doi.org/10.1177/0021998317720009.

[9] Van de Weyenberg I, Chi Truong T, Vangrimde B, Verpoest I. Improving the properties of UD flax fibre reinforced composites by applying an alkaline fibre treatment. Compos A Appl Sci Manuf 2006;37:1368–76. https://doi.org/10.1016/j.compositesa.2005.08.016.

[10] Acera Fernández J. Modification of flax fibres for the development of epoxy-based biocomposites: role of cell wall components and surface treatments on the microstructure and mechanical properties. Université de Montpellier - IMT Mines Alès, 2015.

[11] Seghini MC, Touchard F, Sarasini F, Chocinski-Arnault L, Tirillò J, Bracciale MP, et al. Effects of oxygen and tetravinylsilane plasma treatments on mechanical and interfacial properties of flax yarns in thermoset matrix composites. Cellul 2020;27:511–30. https://doi.org/10.1007/s10570-019-02785-3.

[12] Liotier P-J, Pucci MF, Le Duigou A, Kervoelen A, Tirilló J, Sarasini F, et al. Role of interface formation versus fibres properties in the mechanical behaviour of bio-based composites manufactured by Liquid Composite Molding processes. Compos B Eng 2019;163:86–95. https://doi.org/10.1016/j.compositesb.2018.10.103.

[13] Agarwal BD, Broutman LJ, Chandrashekhara K. Analysis and performance of fiber composites. John Wiley & Sons; 2017.

[14] Téraube O, Agopian J-C, Pucci MF, Liotier P-J, Hajjar-Garreau S, Batisse N, et al. Fluorination of flax fibers for improving the interfacial compatibility of eco-composites. Sustain Mater Technol 2022;33:e00467.

[15] Doineau E. Flax fibres modification by cellulose nanocrystals and xyloglucan for the development of hierarchical biobased composites. IMT Mines Alès; 2020.

[16] Doineau E, Cathala B, Benezet JC, Bras J, Le MN. Development of bio-inspired hierarchical fibres to tailor the fibre/matrix interphase in (Bio)composites. Polymers (Basel) 2021;13:1–34. https://doi.org/10.3390/polym13050804.

[17] Lilli M, Sbardella F, Bavasso I, Bracciale MP, Scheffler C, Rivilla I, et al. Tailoring the interfacial strength of basalt fibres/epoxy composite with ZnO-nanorods. Compos Interfaces 2021;28:771–93. https://doi.org/10.1080/09276440.2020.1805217.

[18] Zabihi O, Ahmadi M, Li Q, Shafei S, Huson MG, Naebe M. Carbon fibre surface modification using functionalized nanoclay: a hierarchical interphase for fibre-reinforced polymer composites. Compos Sci Technol 2017;148:49–58. https://doi.org/10.1016/j.compscitech.2017.05.013.

[19] Chen L, Jin H, Xu Z, Li J, Guo Q, Shan M, et al. Role of a gradient interface layer in interfacial enhancement of carbon fiber/epoxy hierarchical composites. J Mater Sci 2015;50:112–21. https://doi.org/10.1007/s10853-014-8571-y.

[20] Zhuang R-C, Doan TTL, Liu J-W, Zhang J, Gao S-L, Mäder E. Multi-functional multi-walled carbon nanotube-jute fibres and composites. Carbon N Y 2011;49:2683–92. https://doi.org/10.1016/j.carbon.2011.02.057.

[21] Hussain A, Calabria-Holley J, Lawrence M, Ansell MP, Jiang Y, Schorr D, et al. Development of novel building composites based on hemp and multi-functional silica matrix. Compos B Eng 2019;156:266–73. https://doi.org/10.1016/j.compositesb.2018.08.093.

[22] da Silva LJ, Panzera TH, Velloso VR, Christoforo AL, Scarpa F. Hybrid polymeric composites reinforced with sisal fibres and silica microparticles. Compos B Eng 2012;43:3436–44. https://doi.org/10.1016/j.compositesb.2012.01.026.

[23] Wang H, Xian G, Li H. Grafting of nano-TiO2 onto flax fibers and the enhancement of the mechanical properties of the flax fiber and flax fiber/epoxy composite. Compos A Appl Sci Manuf 2015;76:172–80. https://doi.org/10.1016/j.compositesa.2015.05.027.

[24] Asadi A, Miller M, Sultana S, Moon RJ, Kalaitzidou K. Introducing cellulose nanocrystals in sheet molding compounds (SMC). Compos A Appl Sci Manuf 2016;88:206–15. https://doi.org/10.1016/j.compositesa.2016.05.033.

[25] Chen Y, Zhou X, Yin X, Lin Q, Zhu M. A novel route to modify the interface of glass fiber-reinforced epoxy resin composite via bacterial cellulose. Int J Polym Mater Polym Biomater 2014;63:221–7. https://doi.org/10.1080/00914037.2013.830250.

[26] Lee K-Y, Ho KKC, Schlufter K, Bismarck A. Hierarchical composites reinforced with robust short sisal fibre preforms utilising bacterial cellulose as binder. Compos Sci Technol 2012;72:1479–86. https://doi.org/10.1016/j.compscitech.2012.06.014.

[27] Juntaro J, Pommet M, Kalinka G, Mantalaris A, Shaffer MSP, Bismarck A. Creating hierarchical structures in renewable composites by attaching bacterial cellulose onto sisal fibers. Adv Mater 2008;20:3122–6. https://doi.org/10.1002/adma.200703176.

[28] Lee K-Y, Bharadia P, Blaker JJ, Bismarck A. Short sisal fibre reinforced bacterial cellulose polylactide nanocomposites using hairy sisal fibres as reinforcement. Compos A Appl Sci Manuf 2012;43:2065–74. https://doi.org/10.1016/j.compositesa.2012.06.013.

[29] Juntaro J, Pommet M, Mantalaris A, Shaffer M, Bismarck A. Nanocellulose enhanced interfaces in truly green unidirectional fibre reinforced composites. Compos Interfaces 2007;14:753–62. https://doi.org/10.1163/156855407782106573.

[30] Pommet M, Juntaro J, Heng JYY, Mantalaris A, Lee AF, Wilson K, et al. Surface modification of natural fibers using bacteria: depositing bacterial cellulose onto natural fibers to create hierarchical fiber reinforced nanocomposites. Biomacromolecules 2008;9:1643–51. https://doi.org/10.1021/bm800169g.

[31] Ghasemi S, Tajvidi M, Bousfield DW, Gardner DJ. Reinforcement of natural fiber yarns by cellulose nanomaterials: a multi-scale study. Ind Crop Prod 2018;111:471–81. https://doi.org/10.1016/j.indcrop.2017.11.016.

[32] Dai D, Fan M. Green modification of natural fibres with nanocellulose. RSC Adv 2013;3:4659. https://doi.org/10.1039/c3ra22196b.

[33] Sunny T, Pickering KL. Cellulose nanocrystal treatment of aligned short hemp fibre mats for reinforcement in polypropylene matrix composites. Cellul 2021;28:8429–44. https://doi.org/10.1007/s10570-021-04091-3.

[34] Doineau E, Coqueugniot G, Pucci MF, Caro-Bretelle AS, Cathala B, Bénézet J-C, et al. Hierarchical thermoplastic biocomposites reinforced with flax fibres modified by xyloglucan and cellulose nanocrystals. Carbohydr Polym 2021;254:117403. https://doi.org/10.1016/j.carbpol.2020.117403.

[35] Doineau E, Bauer G, Ensenlaz L, Novales B, Sillard C, Bénézet J-C, et al. Adsorption of xyloglucan and cellulose nanocrystals on natural fibres for the creation of hierarchically structured fibres. Carbohydr Polym 2020;248:116713. https://doi.org/10.1016/j.carbpol.2020.116713.

[36] Benselfelt T, Cranston ED, Ondaral S, Johansson E, Brumer H, Rutland MW, et al. Adsorption of xyloglucan onto cellulose surfaces of different morphologies: an entropy-driven process. Biomacromolecules 2016;17:2801–11. https://doi.org/10.1021/acs.biomac.6b00561.

[37] Park YB, Cosgrove DJ. Xyloglucan and its interactions with other components of the growing cell wall. Plant Cell Physiol 2015;56:180–94. https://doi.org/10.1093/pcp/pcu204.

[38] Jeantet L, Regazzi A, Perrin D, Pucci MF, Corn S, Quantin J-C, et al. Recycled carbon fiber potential for reuse in carbon fiber/PA6 composite parts. Compos B Eng 2024;269:111100. https://doi.org/10.1016/j.compositesb.2023.111100.

[39] Pucci MF, Liotier P-J, Seveno D, Fuentes C, Van Vuure A, Drapier S. Wetting and swelling property modifications of elementary flax fibres and their effects on the Liquid Composite Molding process. Compos A Appl Sci Manuf 2017;97:31–40. https://doi.org/10.1016/j.compositesa.2017.02.028.

[40] Garat W, Corn S, Le Moigne N, Beaugrand J, Bergeret A. Analysis of the morphometric variations in natural fibres by automated laser scanning: towards an efficient and reliable assessment of the cross-sectional area. Compos A Appl Sci Manuf 2018;108:114–23. https://doi.org/10.1016/j.compositesa.2018.02.018.

[41] Miller B, Muri P, Rebenfeld L. A microbond method for determination of the shear strength of a fiber/resin interface. Compos Sci Technol 1987;28:17–32. https://doi.org/10.1016/0266-3538(87)90059-5.

[42] Gay D. Matériaux composites, 4ème édition. 4ème édition. Hermès - Lavoisier; 1997.

[43] Balnois E, Busnel F, Baley C, Grohens Y. An AFM study of the effect of chemical treatments on the surface microstructure and adhesion properties of flax fibres. Compos Interfaces 2007;14:715–31. https://doi.org/10.1163/156855407782106537.

[44] Ahmed T, Shahid M, Azeem F, Rasul I, Shah AA, Noman M, et al. Biodegradation of plastics: current scenario and future prospects for environmental safety. Environ Sci Pollut Res 2018;25:7287–98. https://doi.org/10.1007/s11356-018-1234-9.

[45] le Duigou A, Bourmaud A, Balnois E, Davies P, Baley C. Improving the interfacial properties between flax fibres and PLLA by a water fibre treatment and drying cycle. Ind Crop Prod 2012;39:31–9. https://doi.org/10.1016/j.indcrop.2012.02.001.

[46] Raj G, Balnois E, Baley C, Grohens Y. Adhesion force mapping of raw and treated flax fibres using AFM force-volume. J Scan Probe Microsc 2009;4:66–72. https://doi.org/10.1166/jspm.2009.1010.

[47] Felder É, Darque-Ceretti É. Adhésion et Adhérence. CNRS Editions; 2003.

[48] Owens DK, Wendt RC. Estimation of the surface free energy of polymers. J Appl Polym Sci 1969;13:1741–7. https://doi.org/10.1002/app.1969.070130815.

[49] Li S, Li H, Wang X, Song Y, Liu Y, Jiang L, et al. Super-hydrophobicity of large-area honeycomb-like aligned carbon nanotubes. J Phys Chem B 2002;106:9274–6. https://doi.org/10.1021/jp0209401.

[50] Qian H, Bismarck A, Greenhalgh ES, Kalinka G, Shaffer MSP. Hierarchical composites reinforced with carbon nanotube grafted fibers: the potential assessed at the single fiber level. Chem Mater 2008;20:1862–9. https://doi.org/10.1021/cm702782j.

[51] Khoshkava V, Kamal MR. Effect of surface energy on dispersion and mechanical properties of polymer/nanocrystalline cellulose nanocomposites. Biomacromolecules 2013;14:3155–63. https://doi.org/10.1021/bm400784j.

[52] Pirich CL, de Freitas RA, Woehl MA, Picheth GF, Petri DFS, Sierakowski MR. Bacterial cellulose nanocrystals: impact of the sulfate content on the interaction with xyloglucan. Cellul 2015;22:1773–87. https://doi.org/10.1007/s10570-015-0626-y.

[53] Schrader ME. Young-dupre revisited. Langmuir 1995;11:3585–9. https://doi.org/10.1021/la00009a049.

[54] Bangham DH, Razouk RI. Adsorption and the wettability of solid surfaces. Trans Faraday Soc 1937;33:1459. https://doi.org/10.1039/tf9373301459.

[55] Wu S. Polymer Interface and Adhesion. Routledge 2017. https://doi.org/10.1201/9780203742860.

[56] Wu S. Calculation of interfacial tension in polymer systems. J Polym Sci, Part C: Polym Symp 1971;34:19–30. https://doi.org/10.1002/polc.5070340105.

[57] Le Duigou A, Kervoelen A, Le Grand A, Nardin M, Baley C. Interfacial properties of flax fibre–epoxy resin systems: existence of a complex interphase. Compos Sci Technol 2014;100:152–7. https://doi.org/10.1016/j.compscitech.2014.06.009.

[58] Coroller G, Lefeuvre A, Le Duigou A, Bourmaud A, Ausias G, Gaudry T, et al. Effect of flax fibres individualisation on tensile failure of flax/epoxy unidirectional composite. Compos A Appl Sci Manuf 2013;51:62–70. https://doi.org/10.1016/j.compositesa.2013.03.018.

[59] Bourmaud A, Ausias G, Lebrun G, Tachon M-L, Baley C. Observation of the structure of a composite polypropylene/flax and damage mechanisms under stress. Ind Crop Prod 2013;43:225–36. https://doi.org/10.1016/j.indcrop.2012.07.030.

[60] Baley C, Perrot Y, Busnel F, Guezenoc H, Davies P. Transverse tensile behaviour of unidirectional plies reinforced with flax fibres. Mater Lett 2006;60:2984–7. https://doi.org/10.1016/j.matlet.2006.02.028.

[61] Li Y, Li Q, Ma H. The voids formation mechanisms and their effects on the mechanical properties of flax fiber reinforced epoxy composites. Compos A Appl Sci Manuf 2015;72:40–8. https://doi.org/10.1016/j.compositesa.2015.01.029.

[62] Liu L, Zhang B-M, Wang D-F, Wu Z-J. Effects of cure cycles on void content and mechanical properties of composite laminates. Compos Struct 2006;73:303–9. https://doi.org/10.1016/j.compstruct.2005.02.001.

[63] Madsen B, Thygesen A, Lilholt H. Plant fibre composites – porosity and volumetric interaction. Compos Sci Technol 2007;67:1584–600. https://doi.org/10.1016/j.compscitech.2006.07.009.
[64] CELC European Scientific Commitee. Flax and Hemp fibres: a natural solution for the composite industry. JEC Composites; 2012.
[65] Madsen B, Lilholt H. Physical and mechanical properties of unidirectional plant fibre composites—an evaluation of the influence of porosity. Compos Sci Technol 2003;63:1265–72. https://doi.org/10.1016/S0266-3538(03)00097-6.
[66] de Kergariou C, Le Duigou A, Popineau V, Gager V, Kervoelen A, Perriman A, et al. Measure of porosity in flax fibres reinforced polylactic acid biocomposites. Compos A Appl Sci Manuf 2021;141:106183. https://doi.org/10.1016/j.compositesa.2020.106183.
[67] Frącz W, Janowski G, Pruchniak M, Wałek Ł. The use of computed tomography in the study of microstructure of molded pieces made of Poly(3-hydroxybutyric-co-3-hydroxyvaleric acid) (PHBV) biocomposites with natural fiber. Polymers (Basel) 2021;13:2942. https://doi.org/10.3390/polym13172942.
[68] Ramakrishnan KR, Le Moigne N, De Almeida O, Regazzi A, Corn S. Optimized manufacturing of thermoplastic biocomposites by fast induction-heated compression moulding: Influence of processing parameters on microstructure development and mechanical behaviour. Compos A Appl Sci Manuf 2019;124:105493. https://doi.org/10.1016/j.compositesa.2019.105493.
[69] Abida M, Gehring F, Mars J, Vivet A, Dammak F, Haddar M. Hygro-mechanical coupling and multiscale swelling coefficients assessment of flax yarns and flax / epoxy composites. Compos A Appl Sci Manuf 2020;136:105914. https://doi.org/10.1016/j.compositesa.2020.105914.
[70] Saadati Y, Lebrun G, Chatelain J-F, Beauchamp Y. Experimental investigation of failure mechanisms and evaluation of physical/mechanical properties of unidirectional flax–epoxy composites. J Compos Mater 2020;54:2781–801. https://doi.org/10.1177/0021998320902243.
[71] Kersani M, Lomov SV, Van Vuure AW, Bouabdallah A, Verpoest I. Damage in flax/epoxy quasi-unidirectional woven laminates under quasi-static tension. J Compos Mater 2015;49:403–13. https://doi.org/10.1177/0021998313519282.
[72] Cadu T, Berges M, Sicot O, Person V, Piezel B, Van Schoors L, et al. What are the key parameters to produce a high-grade bio-based composite? application to flax/epoxy UD laminates produced by thermocompression. Compos B Eng 2018;150:36–46. https://doi.org/10.1016/j.compositesb.2018.04.059.
[73] Marrot L, Bourmaud A, Bono P, Baley C. Multi-scale study of the adhesion between flax fibers and biobased thermoset matrices. Mater Des (1980–2015) 2014,;62:47–56. https://doi.org/10.1016/j.matdes.2014.04.087.
[74] Oksman K. High quality flax fibre composites manufactured by the resin transfer moulding process. J Reinf Plast Compos 2001;20:621–7. https://doi.org/10.1177/073168401772678634.
[75] Van de Weyenberg I, Ivens J, De Coster A, Kino B, Baetens E, Verpoest I. Influence of processing and chemical treatment of flax fibres on their composites. Compos Sci Technol 2003;63:1241–6. https://doi.org/10.1016/S0266-3538(03)00093-9.
[76] Omrani F, Wang P, Soulat D, Ferreira M. Mechanical properties of flax-fibre-reinforced preforms and composites: Influence of the type of yarns on multi-scale characterisations. Compos A Appl Sci Manuf 2017;93:72–81. https://doi.org/10.1016/j.compositesa.2016.11.013.
[77] Baley C, Le Duigou A, Bourmaud A, Davies P. Influence of drying on the mechanical behaviour of flax fibres and their unidirectional composites. Compos A Appl Sci Manuf 2012;43:1226–33. https://doi.org/10.1016/j.compositesa.2012.03.005.
[78] César dos Santos J, Ávila de Oliveira L, Panzera TH, Remillat CDL, Farrow I, Placet V, et al. Ageing of autoclaved epoxy/flax composites: Effects on water absorption, porosity and flexural behaviour. Compos B Eng 2020;202:108380. https://doi.org/10.1016/j.compositesb.2020.108380.
[79] Hallak Panzera T, Jeannin T, Gabrion X, Placet V, Remillat C, Farrow I, et al. Static, fatigue and impact behaviour of an autoclaved flax fibre reinforced composite for aerospace engineering. Compos B Eng 2020;197:108049. https://doi.org/10.1016/j.compositesb.2020.108049.
[80] Rayyaan R, Kennon WR, Potluri P, Akonda M. Fibre architecture modification to improve the tensile properties of flax-reinforced composites. J Compos Mater 2020;54:379–95. https://doi.org/10.1177/0021998319863156.
[81] Bergeret A, Krawczak P. Liaison renfort/matrice. Techniques de l'ingénieur Plastiques et. Composites 2006.
[82] Le Duigou A, Davies P, Baley C. Exploring durability of interfaces in flax fibre/epoxy micro-composites. Compos A Appl Sci Manuf 2013;48:121–8. https://doi.org/10.1016/j.compositesa.2013.01.010.